Supplemental Figures

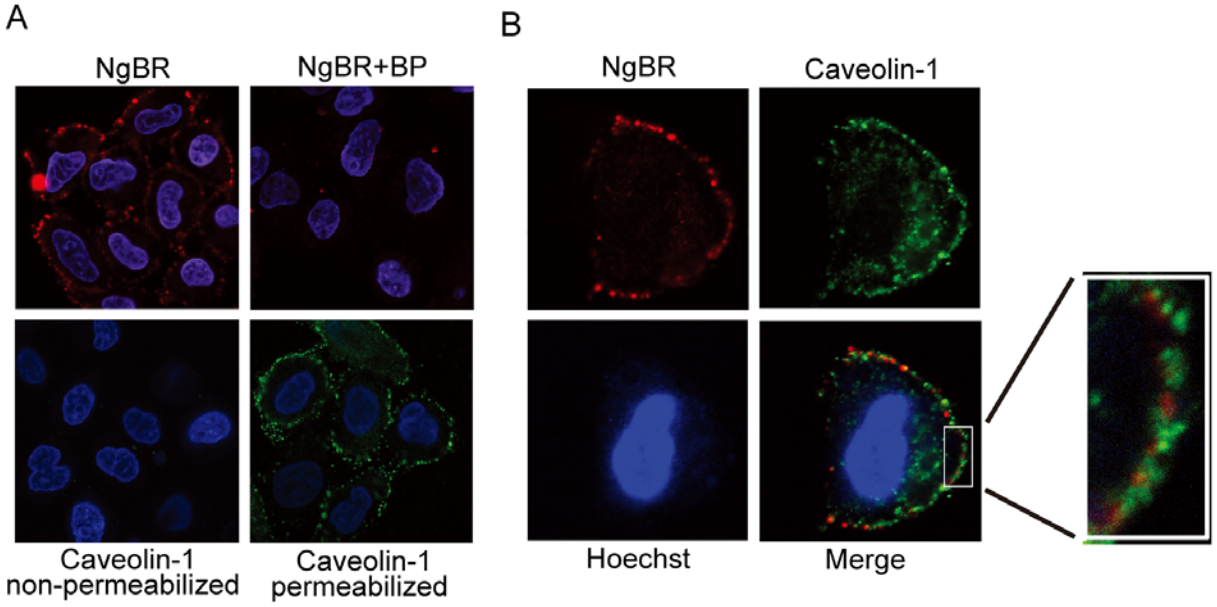

Figure S1. NgBR is localized in non-Caveolin-1 regions in the plasma membrane. (A) Fluorescence immunostaining of NgBR on the non-permeabilized HeLa cells can be blocked by the peptide derived from the same epitope of NgBR recognized by NgBR antibody. Non-permeabilization of HeLa cells was confirmed by fluorescence immunostaining of Caveolin-1. BP: blocking peptide of NgBR antibody. (B) NgBR is not co-localized with Caveolin-1 in HeLa cell plasma membranes, as determined by fluorescence immunostaining. NgBR and caveolin-1 were labeled by red fluorescence (Alexa Fluor 568 Donkey Anti-Rabbit IgG) and green fluorescence (Alexa Fluor 488 Donkey Anti-Mouse IgG), respectively.

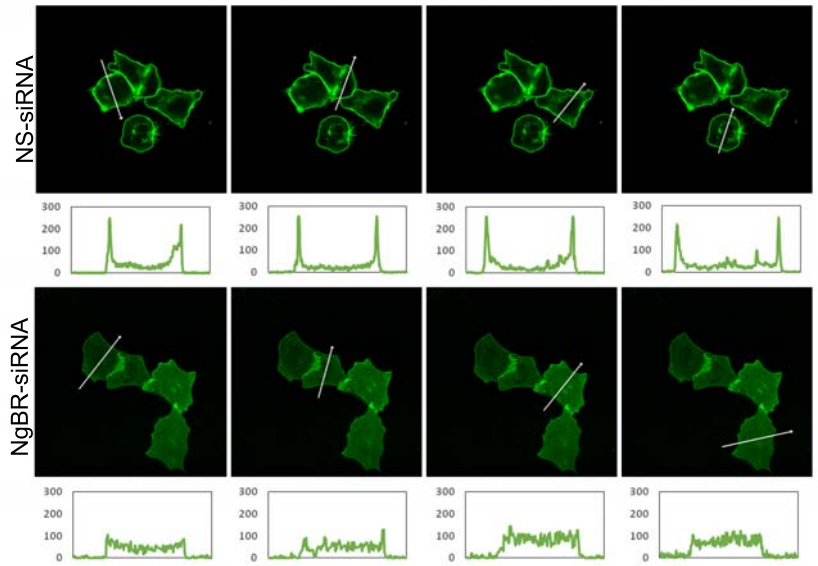

Figure S2. The intensity of EGFP-H-Ras fluorescence signal across the three-dimensional reconstruction of the z-stack image. Three dimensional reconstruction of the z-stack image was performed using shadow rendering method included in 4D module of Axiovision 4.8 software (Carl Zeiss, Jena, Germany). Intensity threshold and brightness scales were set to highlight the data above the baseline values to represent EGFP-H-Ras positive membrane signal. Identical settings were used for comparing NS-siRNA and NgBR-siRNA samples for data collection and data analysis (Axiovision). For analyzing the membrane localization and distribution of protein, a line was drawn across a cell (outside of the nucleus) using profile tool in AIM software. This plots the intensity of the pixels along the line that represents plasma membrane and cytoplasm distribution of EGFP signal. A spike of the fluorescence intensity at the plasma membrane and lower intensity (close to baseline) across the cytoplasm indicate plasma membrane localization. A flat line distribution represents non-membrane specific distribution in NgBR depletion cells. Data collection and analysis between NS-siRNA and NgBR-siRNA samples were carried out under identical conditions.

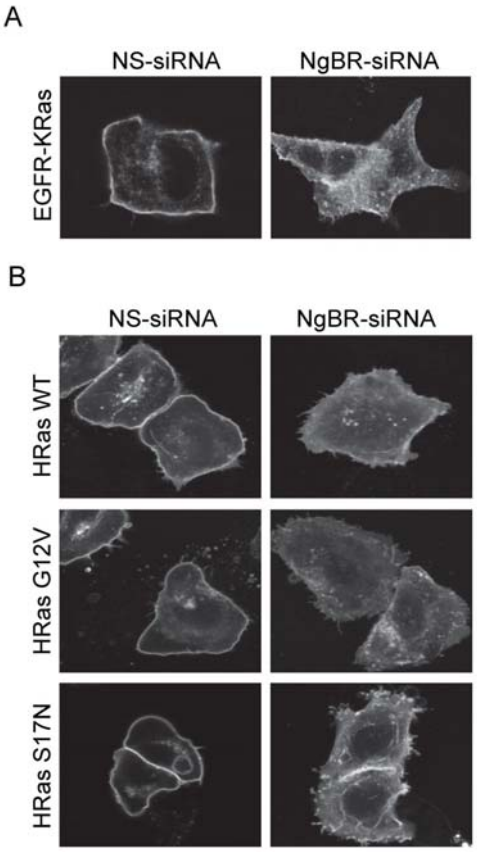

Figure S3. NgBR promotes the plasma membrane accumulation of EGFP-K-Ras as well as GDP/GTP-loaded EGFP-H-Ras in HeLa cells. (A) NgBR knockdown impaired the plasma membrane localization of EGFP-K-Ras in HeLa cells. (B) NgBR knockdown impaired the plasma membrane localization of GDP/GTP-loaded EGFP-H-Ras in HeLa cells. EGFP-H-Ras-S17N is the dominant negative H-Ras mutant that does not bind GTP. EGFP-H-Ras-G12V is the GTP-loaded constitutively active H-Ras mutant. NgBR was knocked down by using siRNA.

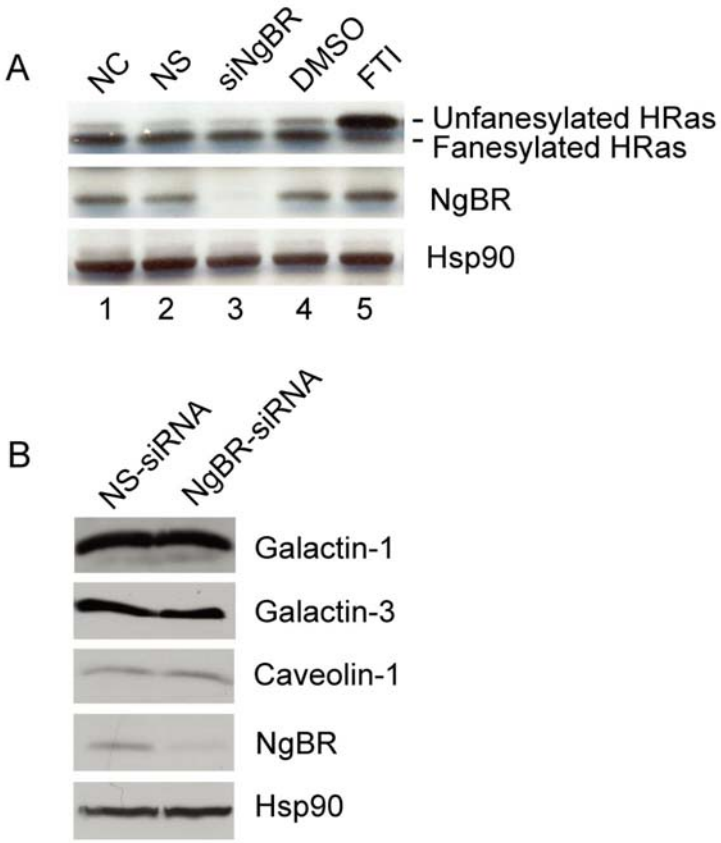

Figure S4. NgBR knockdown does not change the expression of known proteins associated with Ras translocation and farnesylation of Ras. (A) NgBR knockdown does not affect the farnesylation of H-Ras. FTI: the farnesylation inhibitor. (B) NgBR knockdown does not affect the expression of Galactin-1, 3 and Caveolin-1. Protein levels were determined by Western blotting. NgBR was knocked down by using siRNA.

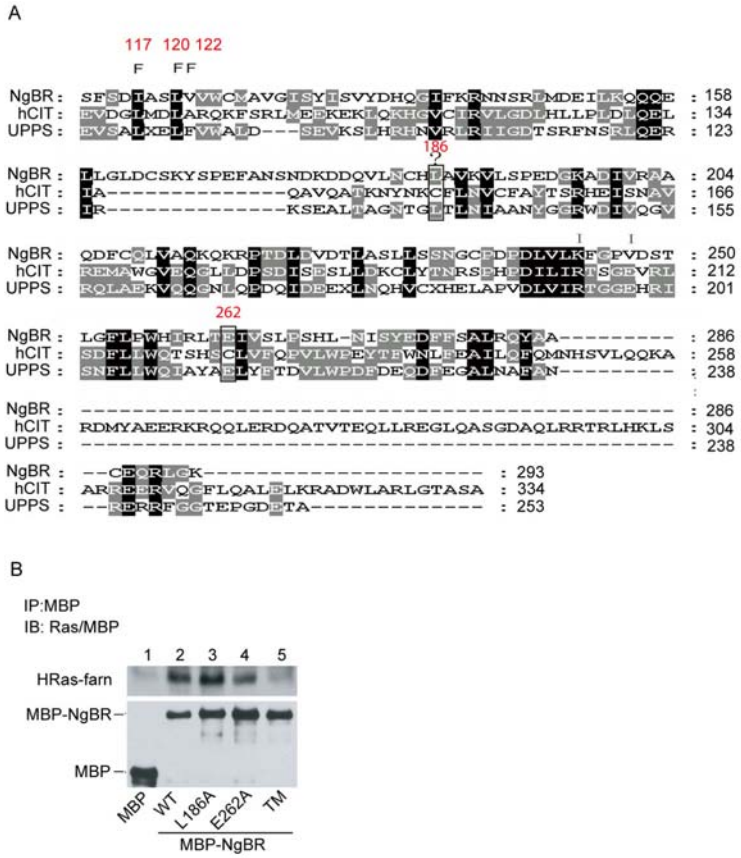

Figure S5. Identification of critical residues of NgBR essential for the binding of NgBR to Ras. (A) Alignment of NgBR, hCIT (human cis-isoprenyltransferase) and UPPS (E. coli undecaprenyl diphosphate synthase). The residues labeled with red font are potentially critical AA needed for the binding of NgBR to Ras. (B) Mutation of critical AA residues of NgBR reduces the binding of NgBR to Ras. Purified recombinant proteins of MBP-NgBR and H-Ras were incubated at room temperature for 1 hour and complexes were pulled down using anti-MBP beads. Protein levels were detected by Western blotting.

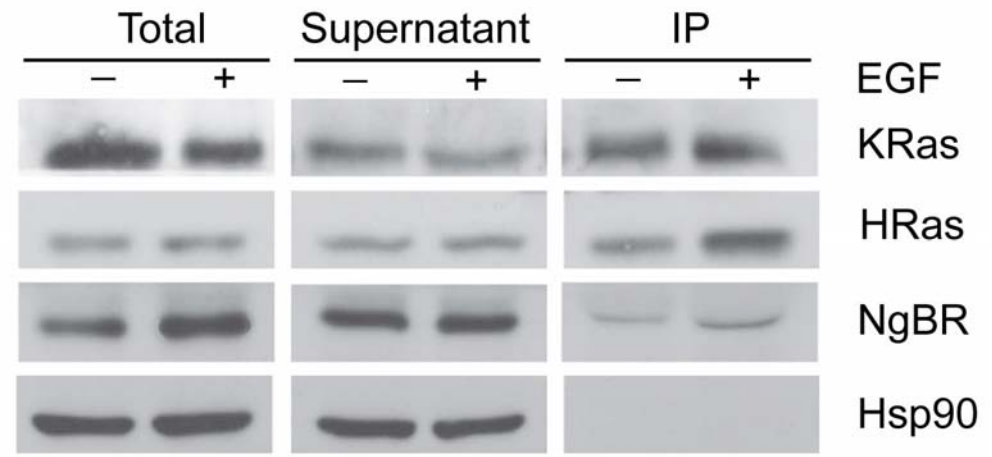

Figure S6. NgBR interacts with activated H-Ras in NIH-3T3 cells overexpressing NgBR-HA. The complex of activated Ras (GTP-loaded Ras) was precipitated from quiescent cells stimulated with or without EGF (10 ng/ml for 5 minutes) using GST-RBD beads. Protein levels were detected by Western blotting. Both Ras and NgBR were detected in the complexes precipitated by the Raf-pull-down method.

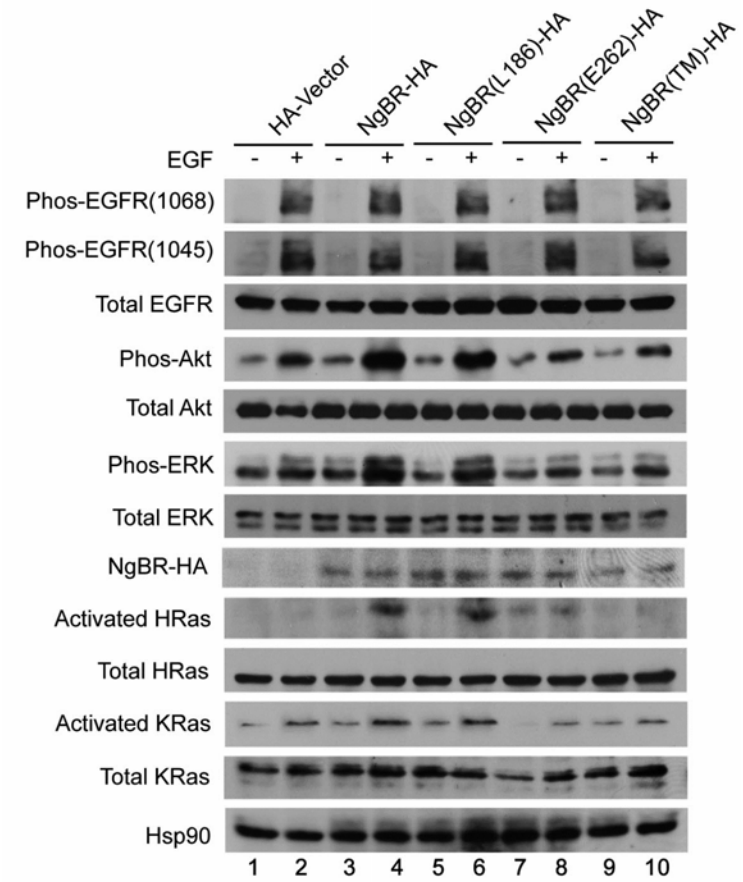

Figure S7. Effects of NgBR mutants on EGF-stimulated Ras activation and signaling in NIH-3T3 cells. Plasmid DNA of wild-type NgBR-HA or mutants was transfected to NIH-3T3 cells, respectively. After 24 hour after transfection, cells were arrested overnight in serum-free medium and then stimulated with 10 ng/ml EGF for 10 minutes. The activated Ras proteins were isolated using GST-RBD beads. The EGF-induced activation of H-Ras and K-Ras was determined by Western blotting. Phosphorylation of Akt and ERK was determined by Western blotting using phosphorylation specific antibodies.

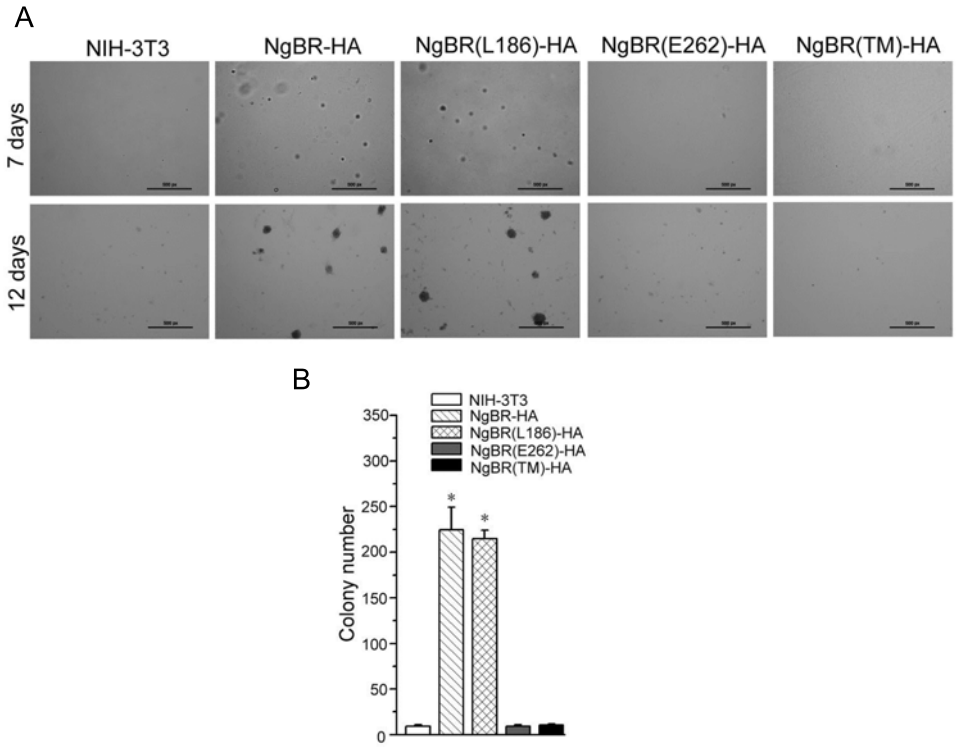

Figure S8. Effects of NgBR mutants on the colony formation of NIH-3T3 cells. Plasmid DNA of wild-type NgBR-HA or mutants was transfected to NIH-3T3 cells, respectively. After 24 hour after transfection, cells were seed in soft agar. Images of colony formation of NIH-3T3 cells (A) and quantification of the results (B) are shown. Data are represented as mean ± SEM (* $P < 0.05$, $n=3$).

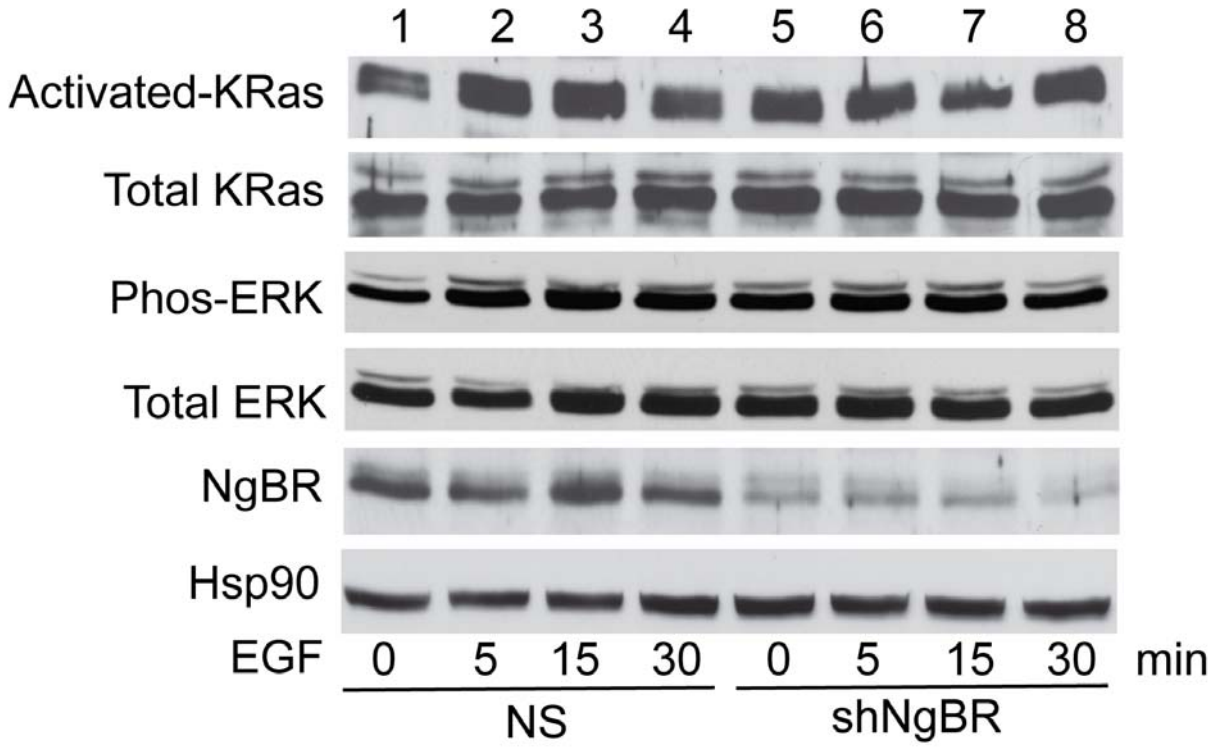

Figure S9. (A) NgBR knockdown does not affect the EGF induced activation of K-Ras in MDA-MB-231 cells. NgBR were knocked down by using shRNA. Protein levels were detected by Western blotting.

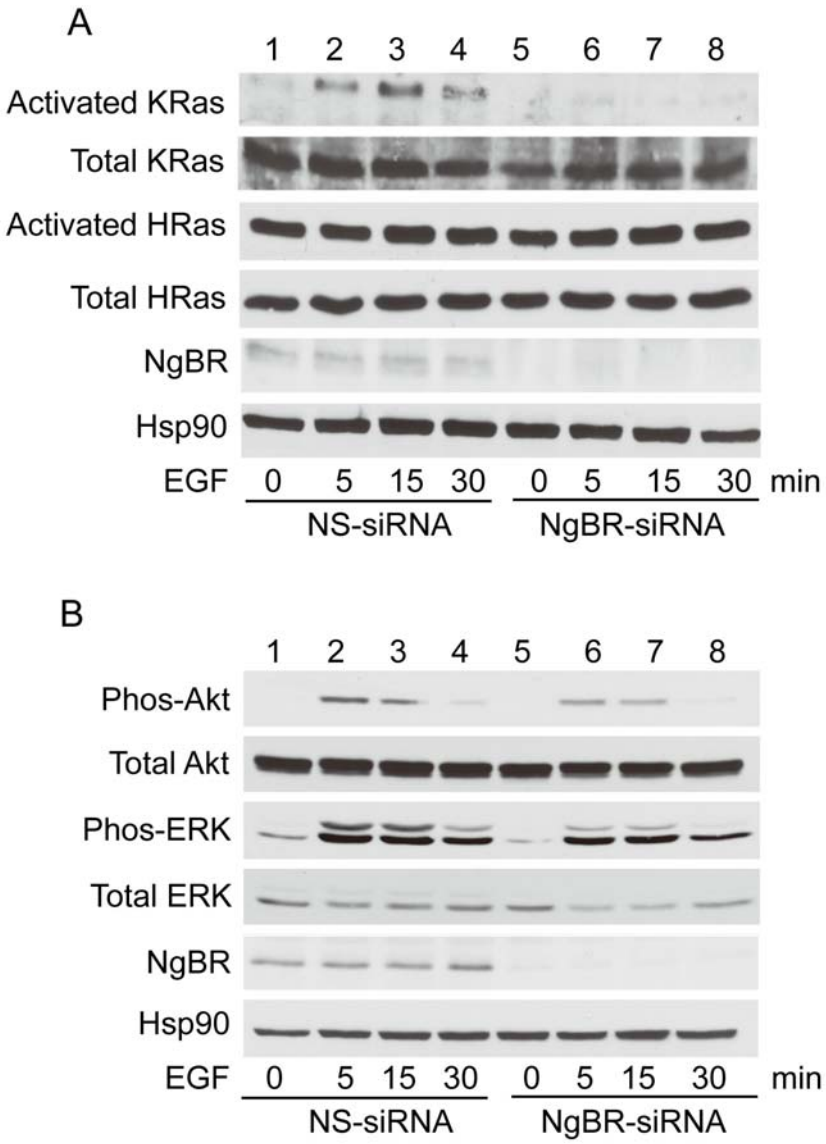

Figure S10. (A) NgBR knockdown reduces the EGF induced activation of K-Ras but not H-Ras in T24 cells. (B) NgBR knockdown reduces the EGF induced phosphorylation of Akt and Erk in T24 cells. NgBR was knocked down by using siRNA. Protein levels were detected by Western blotting.

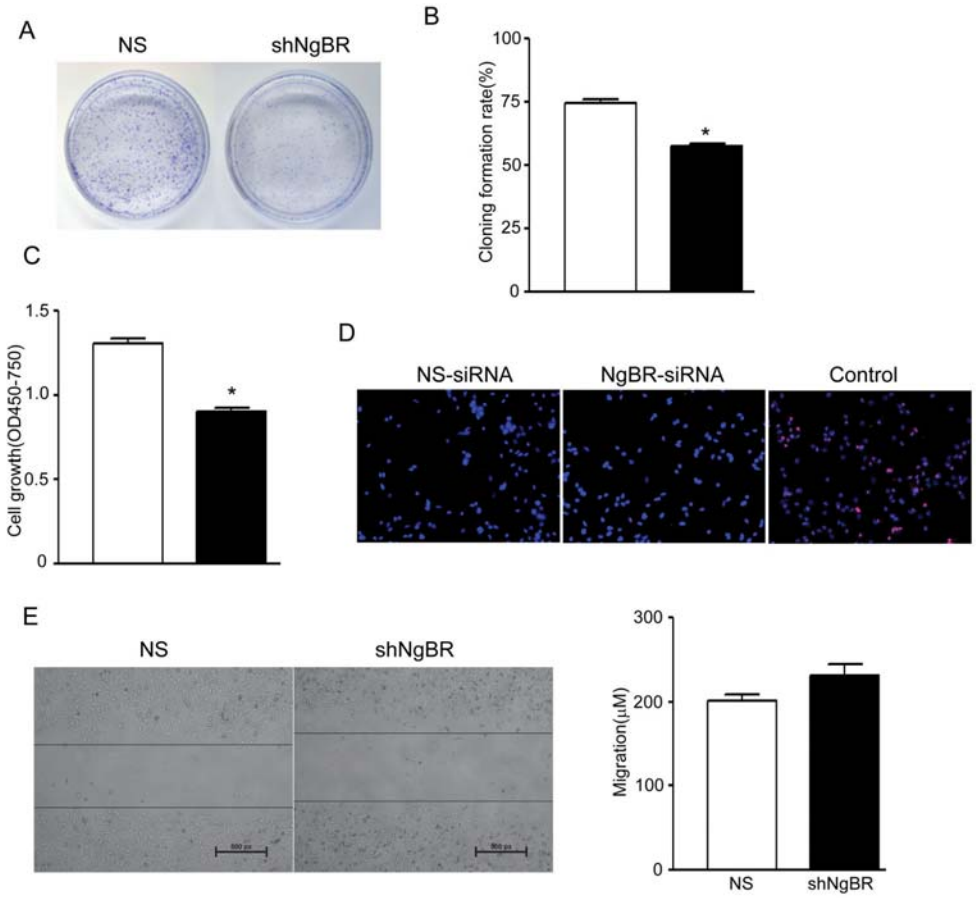

Figure S11. (A-B) NgBR knockdown reduces the colony formation of MDA-MB-231 cells. Visualization (A) and quantification results (B) of MDA-MB-231 cell colony formation. Data are represented as mean ± SEM (* *P*< 0.05, n=3). **(C) NgBR knockdown reduces the growth of MDA-MB-231 cells.** Data are represented as mean ± SEM (* *P*< 0.05, n=3). **(D) NgBR knockdown does not induce the apoptosis of MDA-MB-231 cells.**Positive control group is MDA-MB-231 cells treated with cisplatin. The apoptotic cells were determined by TUNEL staining. **(E-F) NgBR knockdown does not affect the migration of MDA-MB-231 cells.** Visualization (E) and quantification results (F) of migrating cells. Stable MDA-MB-231 cell lines having either NS or NgBR shRNAi were established by using puromycin selection. Data are represented as mean ± SEM (n=3).

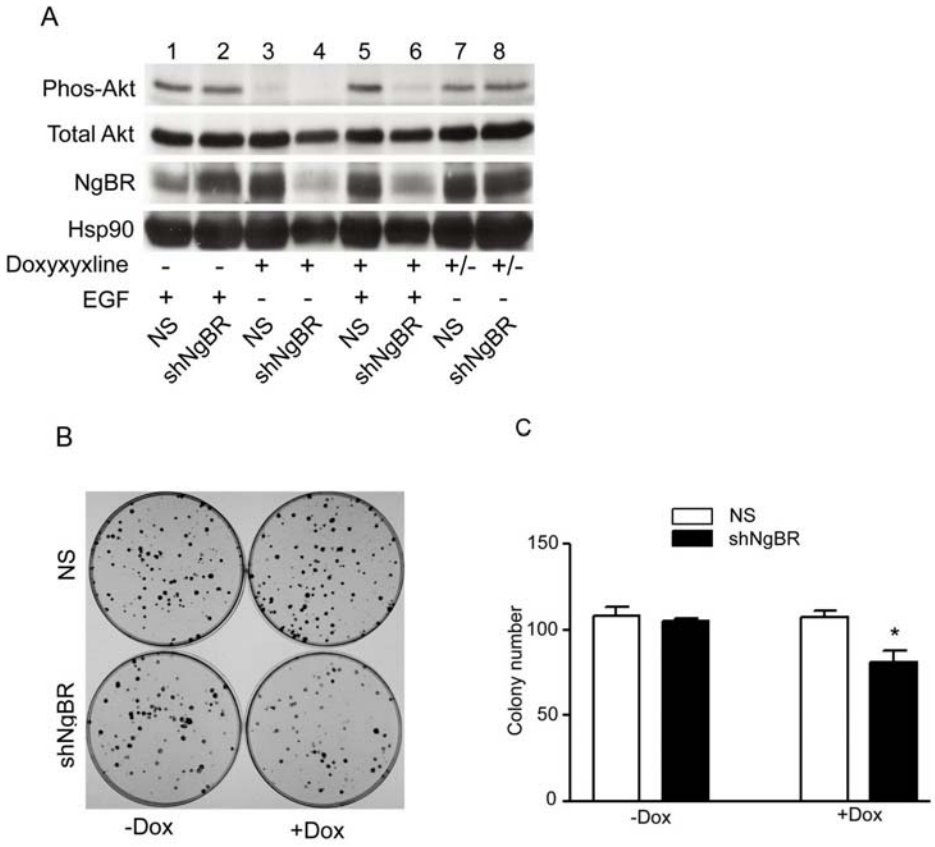

Figure S12. Inducible knockdown of NgBR reduces the expression of NgBR in MDA-MB-231 shNgBR stable cell lines. (A) Doxycycline treatment induces NgBR knockdown and reduces EGF induced phosphorylation of Akt in MDA-MB-231 shNgBR stable cell lines. NgBR and phosphorylated Akt levels were detected by Western blotting. (B/C) Doxycycline treatment reduces the colony formation of MDA-MB-231 shNgBR stable cell lines but not control NS stable cell lines. Visualization (left panel) and quantification results (right panel) of MDA-MB-213 cell colony formation. Data are represented as mean ± SEM (* $P< 0.05$, n=3).

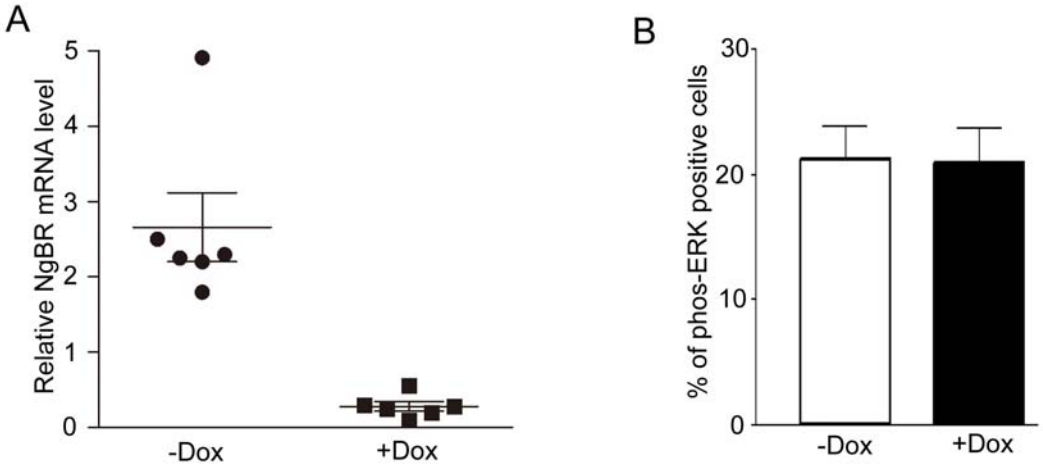

Figure S13 (A) Doxycycline treatment induces NgBR knockdown in MDA-MB-231 shNgBR tumor xenograft. NgBR expression levels were detected by real-time PCR. Data are represented as mean ± SEM (* $P < 0.05$, n=6). **(B) Inducible knockdown of NgBR does not affect the phosphorylation of Erk in MDA-MB-231 shNgBR tumor xenografts.** NgBR was knocked down by feeding the mice with doxycycline in drinking water. Phosphorylation of Erk was determined by immunostaining using specific phosphorylation antibodies. Data are represented as mean ± SEM (n=4).

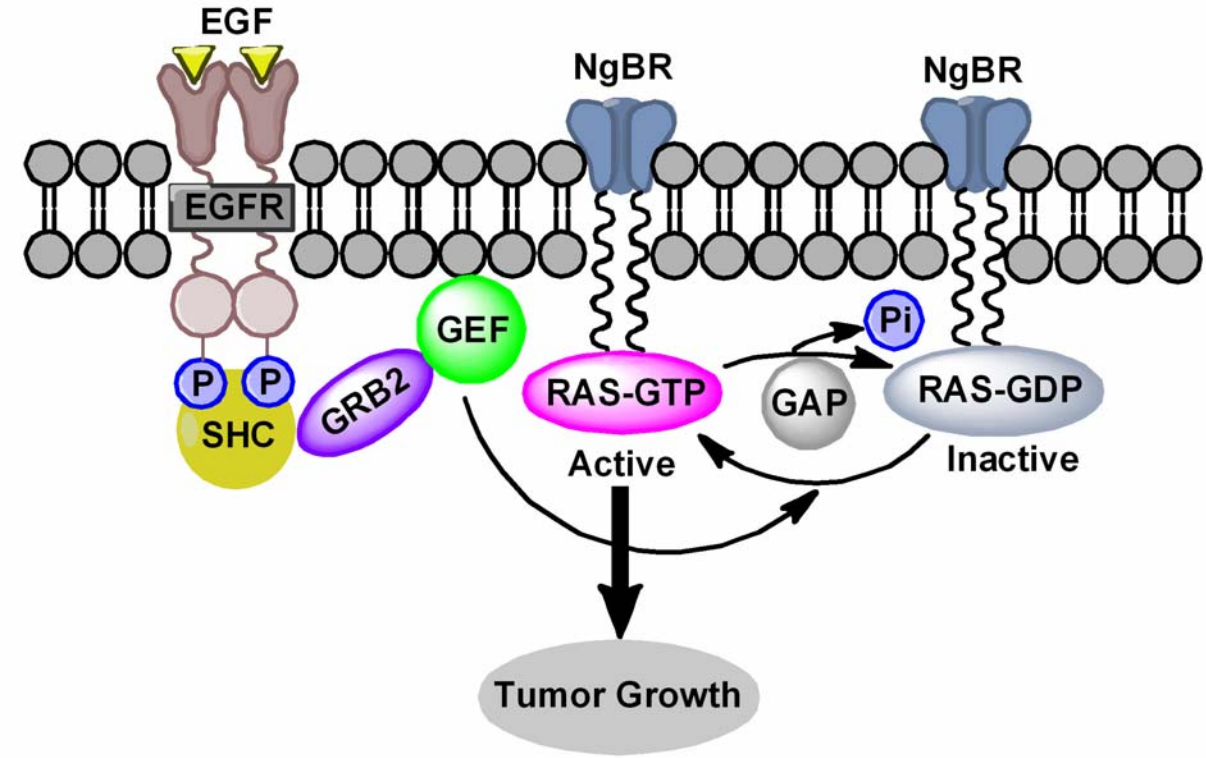

Figure S14. NgBR is essential for Ras plasma membrane translocation and promotes tumorigenesis. EGF binds the EGF receptor (EGFR) to recruit RasGEFs such as SOS via its SHC domain and Grb2 adapter protein. NgBR promotes Ras plasma membrane translocation and enhances EGF signaling by providing more plasma membrane associated Ras.